National Aeronautics and Space Administration

LiDAR-Inertial Based Navigation and Mapping for Precision Landing

Principal Investigator: Timothy Setterfield (343); Co-Investigators: Robert Hewitt (347), Po-Ting Chen (343), Nikolas Trawny (343), Anup Katake (343), Corey Marcus (343)

Program: FY21 R&TD **Strategic Focus Area: Precision Landing**

Objectives

The objective of this R&TD was to develop, mature, and demonstrate a 3D Light Detection and Ranging (LiDAR) based, illumination-insensitive navigation and mapping algorithm that ensures safe and precise landing on planetary bodies, e.g., Europa, Enceladus, Mars, the Moon, and small bodies. In FY20, the requisite algorithms were developed and tested on simulated dense LiDAR data. The objective of our efforts in FY21 were to advance the TRL of the system by demonstrating its functionality with real-world flight data obtained during the Autonomous Landing Hazard Avoidance Technology (ALHAT) program (in 2009 and 2014) and during the Mars 2020 entry, descent and landing (EDL). Accomplishing this objective required that we address further challenges associated with real-world data, such as time synchronization, outlier rejection, poor sensor calibration, and faulty measurements. Additionally, in order to use data from the ALHAT 2009 flight campaign and Mars 2020 EDL, our algorithms needed to be modified to accommodate sparse, as opposed to dense, ranging data.

Background

Future JPL lander missions to Europa, Enceladus, comets, asteroids, or permanently shadowed regions of the Moon will face several new challenges. Limited topographic information about the surface will be available prior to descent. Hazards will need to be mapped autonomously. Sites of the greatest scientific interest will be near extreme terrain, requiring precision landing. Landing when illumination conditions are similar to those during initial surface mapping, which was a requirement for the camera-based Lander Vision System (LVS) used on Mars 2020, may be impractical. 3D LiDAR provides ranging over an entire field of points, which can be used for both localization and mapping; unlike a camera, it provides direct, high-confidence depth measurements, and is invariant to lighting conditions. Together with an inertial measurement unit (IMU), LiDAR can be used to replace or augment a traditional landing sensor suite, and enable safe and precise landing in the face of the aforementioned challenges.

Approach and Results

The algorithmic approach to LiDAR-inertial based navigation was to estimate the maximum a posteriori trajectory (pose, velocity, and IMU biases at the start of each LiDAR scan) using incremental smoothing. Several probabilistic factors are input to an optimization algorithm, with each relying on a different measurement technique: inertial odometry, which pre-integrates several IMU measurements to constrain temporally adjacent lander states; LiDAR-odometry, which estimates motion by matching features in temporally adjacent range and intensity images (Figure 2a); and map relative localization (MRL), which localizes the lander by matching measured LiDAR scans to digital elevation models (DEMs) obtained previously from orbit (Figure 2b). The estimated trajectory is then used to re-project LiDAR range measurements into the existing DEM, refining the map to higher resolutions suitable for onboard safe landing site selection. The resultant map is also useful for science operations planning and analysis of surface structure.

National Aeronautics and Space Administration

Jet Propulsion Laboratory
California Institute of Technology
Pasadena, California

www.nasa.gov

PI/Task Mgr Contact
Email: timothy.p.setterfield@jpl.nasa.gov

Measurement data from ALHAT and Mars 2020 were formatted into generic ASCII files in order to be replayed with our algorithms. Several issues with the ALHAT field test data, such as instrument time synchronization and ranging biases, were corrected. ALHAT flight test (FT) 3 data is from a laser altimeter attached to an airplane flying 2-8 km above Yucca Flats and Death Valley in 2009 (Figure 1a). ALHAT FT6 data is from a 128×128-pixel flash LiDAR flying 250-0 m over an artificial boulder field on a Morpheus vertical takeoff and landing rocket at Kennedy Space Center (Figure 1b). Mars 2020 data is from a six-beam terminal descent sensor (TDS) radar during descent from 10-0 km on Mars in 2021 (Figure 1c). While the high-quality IMU data for ALHAT FT6 and Mars 2020 EDL was sufficient for integration over the relatively short descents (40 and 152 seconds respectively), this was not the case for accelerometer integration during the long ALHAT FT3 flights (each up to 2.3 hours). For these flights, data from a simulated velocimeter, measuring velocity in the local body frame, was added. For ALHAT FT3 and Mars 2020 data, several range measurements were binned together to form a sparse contour. To address the sparsity of the resulting ground-projected scans, we modified our MRL correlator to mask unoccupied pixels.

Estimates of position and velocity for ALHAT FT6 Free Flight 14 are shown in Figure 3. A clear advantage of estimating the entire trajectory is that once the instantaneous estimated position and velocity (dashed lines) lock on to accurate values, all previous smoothed estimates are corrected (dotted lines). This allows LiDAR data obtained before the state was well-estimated to be incorporated into the onboard map. Rejecting outliers from real-world data was a major focus of FY21. Figure 4 shows how in ALHAT FT3 Flight 5, a series of seven heuristic tests was able to reject all measurements with errors greater than 200 m when matching to a 5 m/px map. Processing the Mars 2020 data and selecting landing sites from the generated map are ongoing topics of our research; initial results have been promising.

Significance/Benefits to JPL and NASA

We have demonstrated our LiDAR navigation and mapping algorithms on a diverse set of real-world data. In the process, we have made our system more robust and extended its capabilities, allowing it to process sparse, as well as dense, ranging data. For missions to destinations other than the Moon and Mars, orbital topographic information is insufficient for safe landing, and scanning LiDARs will likely be included for hazard detection and avoidance. The software from this R&TD vastly expands the utility of carrying such a LiDAR, enabling not just hazard mapping at a single altitude, but also localization, velocimetry, and continuous hazard mapping at a range of altitudes. For missions to partially or fully shaded destinations, or any missions wishing to avoid restrictions on the time of day of the landing, our LiDAR-based navigation offers an illumination-insensitive replacement to the current state-of-the art visual terrain relative navigation. As we demonstrated by processing contour data, this can even be accomplished at high altitude using only altimetry. This technology could expand the set of reachable destinations in the solar system, and help eliminate the need for costly precursor orbital missions, which are typically required to build maps for localization and landing site selection.

Publications

[A] T. P. Setterfield et al., “LiDAR-Inertial Based Navigation and Mapping for Precision Landing,” IEEE Aero Conf, Big Sky, MT, 2021.
[B] T. P. Setterfield et al., “Real-World Testing of LiDAR-Inertial Based Navigation and Mapping for Precision Landing,” submitted to IEEE Aero Conf, Big Sky, MT, 2022.

Figure 1. Input Data. True trajectories are shown as red lines, projected range measurements as green points.

(a) ALHAT FT3 Flight 5 in a King Air B200 airplane at Yucca Flats with 40.78×73.2 km, 5m/px map, 3.3 to 4.7 km altitude, and LaRC laser altimeter at 30 Hz.

(b) ALHAT FT6 Free Flight 14. Morpheus VTOL rocket at Kennedy Space Center with 186.5×186.5 m, 10 cm/px map, 250 to 85 m altitude, and ASC Goldeneye 128×128 px flash LiDAR at 20 Hz.

(c) Mars 2020 EDL at Jezero Crater with 30×30 km, 24 m/px map, 10 to 0 km altitude, and terminal descent radar with 6 beams at 20 Hz.

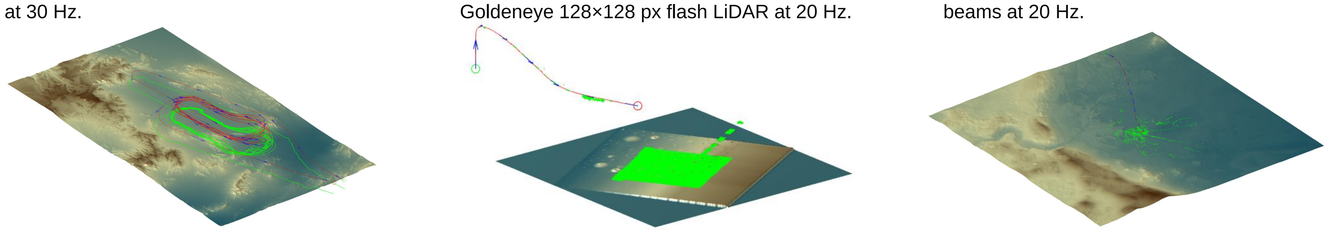

Figure 2. Image Processing (ALHAT FT6 Free Flight 14)

(a) Visual features are tracked frame-to-frame in range (left) and intensity (right) images in for LiDAR odometry.

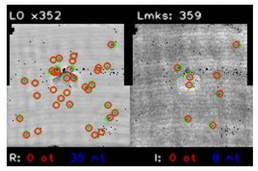

(b) Scan elevation maps (top-left) are correlated to a prior topographic map (center), producing a correlation map (right) for map relative localization.

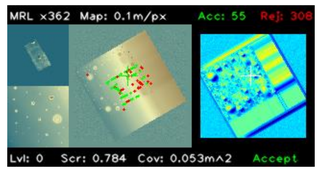

Figure 4. Outlier Rejection (ALHAT FT3 Flight 5)

Outlier rejection on map relative localization of contours was performed by sequentially applying thresholds on several heuristic predictors of large matching error.

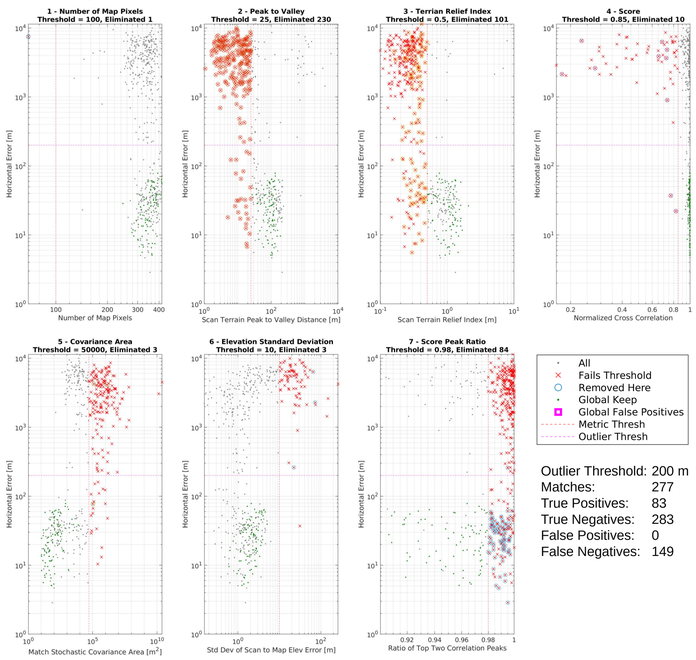

Outlier Threshold: 200 m
Matches: 277
True Positives: 83
True Negatives: 283
False Positives: 0
False Negatives: 149

Figure 3. Estimation (ALHAT FT6 Free Flight 14)

Measurements from LiDAR-inertial odometry and map relative localization (MRL) that pass through outlier rejection are input into a smoothing-based navigation algorithm. The instantaneous estimate and smoothed solution are shown, with convergence occurring at approximately 3.5 seconds for velocity (b) and 11.1 seconds for position (a).

(a)

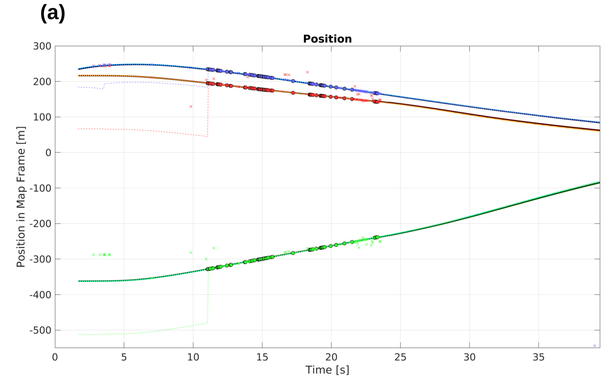

(b)

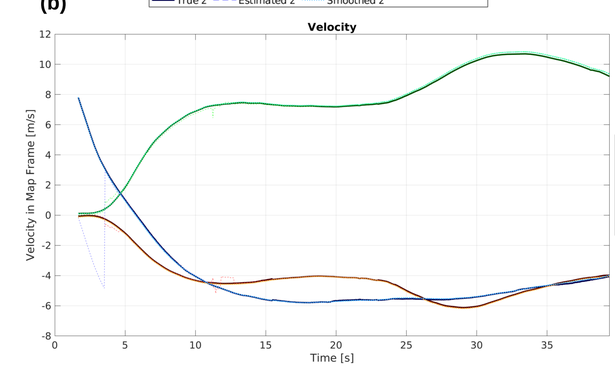

Poster No. R20104
Clearance No.
JPLTask#R20104